Nonrigid Autofocus Motion Correction for Coronary MR Angiography with a 3D Cones Trajectory

R Reeve Ingle[1], Holden H. Wu[2], Nii Okai Addy[1], Jieying Luo[1], Joseph Y. Cheng[1], Phillip C. Yang[3], Bob S Hu[1,4], and Dwight G Nishimura[1]

[1]*Electrical Engineering, Stanford University, Stanford, California, United States,* [2]*Radiological Sciences, UCLA, California, United States,* [3]*Cardiovascular Medicine, Stanford University, Stanford, California, United States,* [4]*Palo Alto Medical Foundation, Palo Alto, California, United States*

Introduction Respiratory motion of the heart is a significant challenge to coronary magnetic resonance angiography (CMRA). Retrospective correction techniques have gained popularity due to their high scan efficiencies, but the effectiveness of these techniques depends on the accuracy with which the motion of the heart can be measured and corrected. Recent autofocusing techniques have combined navigator-based motion compensation with a focusing-metric-based optimization to yield additional suppression of motion artifacts[1,2]. In this work, we present a nonrigid autofocus correction technique for CMRA that uses localized translation measurements from 2D or 3D image navigators (iNAVs) acquired every heartbeat in a 3D cones free-breathing CMRA sequence[3,4]. In volunteer and patient studies, the proposed nonrigid correction technique increases vessel sharpness and improves the depiction of coronary arteries.

Methods Free-breathing CMRA of healthy volunteers and patients was conducted at 1.5 T using an image-navigated 3D cones sequence[3]. Superior-inferior (SI), anterior-posterior (AP), and right-left (RL) translations of the heart were measured using either two orthogonal 2D iNAVs (3.1-mm-resolution sagittal and coronal 2D spiral acquisitions)[3] or one 3D iNAV (4.4-mm-resolution variable-density 3D cones acquisition)[4] acquired every heartbeat. The acquired high-resolution CMRA data were reconstructed with 3D translational rigid-body correction and with nonrigid autofocus motion correction[1,5]. The autofocus correction technique used a set of candidate motion trajectories to reconstruct a bank of rigid-body motion-compensated 3D images. A final nonrigid motion-corrected image was generated in a pixel-by-pixel fashion, using a gradient-entropy focusing metric[6] to select the best-focused pixels from this bank of images. The candidate motion trajectories were derived in one of two ways, depending on the iNAV type (2D or 3D). With 2D iNAVs, mutual-information maximization was used to measure bulk SI, AP, and RL translational motion within a rectangular region of interest (ROI) covering the heart. Candidate motion waveforms were derived by scaling these measured trajectories using nine SI, nine AP, and five RL scale factors evenly spaced between 0x and 2x (405 total combinations)[5]. With 3D iNAVs, nonrigid registration was used to co-register all iNAVs to a single reference iNAV, yielding SI, AP, and RL 3D spatial deformation fields at each heartbeat. A total of 36 candidate motion waveforms were derived from these deformation fields by computing the average SI, AP, and RL translation within 36 different spatially localized ROIs in the heart (1 whole-heart, 2^3 octants, and 3^3 local ROIs). One "static" waveform (i.e., no motion) was also included for reconstruction of non-moving structures. CMRA images were acquired with either a 1.25-mm isotropic-resolution 3D cones readout[3] or a 0.8-mm isotropic-resolution 3D cones readout[7]. Maximum intensity projection (MIP) coronary images reconstructed with no correction, translational correction, and autofocus correction were assigned integer rank scores (1=best, 3=worst) by two cardiologists to compare depiction of each of the three major vessel trees in five subjects.

Results Measured motion trajectories from 2D iNAVs and the scaled versions used by the autofocus algorithm show cyclic respiratory motion during the free-breathing acquisition (Fig. 1). Short-axis reformats from a patient study are shown for two of the 405 images in the reconstruction bank (Figs. 2a-2b). Motion blurring is significantly reduced in Fig. 2b, which was reconstructed with 1x scaling of the measured SI, AP, and RL trajectories, compared to Fig. 2a, which used 0x scaling (no correction). The nonrigid autofocus-corrected image (Fig. 2c) yields additional reduction of motion blurring artifacts, and the SI motion map (Fig. 2d) shows the optimal SI scale factors selected by the algorithm. Reformatted MIPs from a 1.25-mm-resolution patient scan (Fig. 3a) and from a 0.8-mm-resolution patient scan (Fig. 3b) show improvements in the depiction of the left anterior descending (LAD) artery with the 2D iNAV autofocus correction technique. Mean rank scores improved from 2.9±0.3 (no correction) to 2.0±0.4 (translational correction) to 1.1±0.3 (autofocus correction). The 3D iNAV autofocus technique also yields improved depiction of the right coronary artery (RCA) in a 1.25-mm isotropic-resolution volunteer study (Fig. 4).

Discussion & Conclusion The proposed autofocus technique substantially reduced motion blurring and improved the depiction of coronary arteries in free-breathing volunteer and patient CMRA acquisitions. The scaling approach used with 2D iNAVs involved a larger search space than the targeted ROI approach used with 3D iNAVs (405 vs. 37 motion paths), requiring 11x more computation time. Further correction could be feasible by extending the search space using, for example, more complicated models or a combination of the scaling and targeted-ROI methods. In addition to 3D cones CMRA acquisitions, the autofocus technique could be applied to other navigated CMRA acquisitions for retrospective nonrigid motion correction.

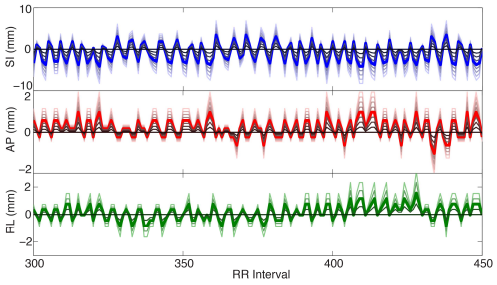

Figure 1. Candidate SI, AP, and RL motion trajectories are derived from iNAVs by scaling a single bulk measurement of the heart (above) or by measuring motion within targeted ROIs (not shown). A bank of motion-corrected 3D images is generated.

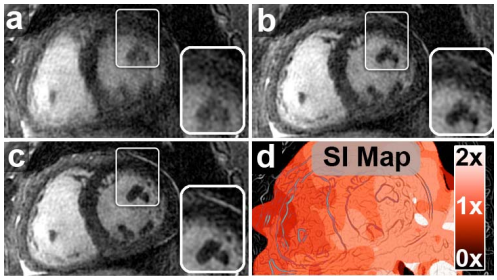

Figure 2. Short-axis reformats from a patient study. The bank of motion-corrected images includes **(a)** no compensation (0x scale) and **(b)** the measured bulk translational compensation (1x scale). **(c)** The final image is assembled using a focusing metric to select the best-focused pixels, improving image sharpness (insets). **(d)** The derived SI motion map shows the SI scale factors selected by the autofocus algorithm.

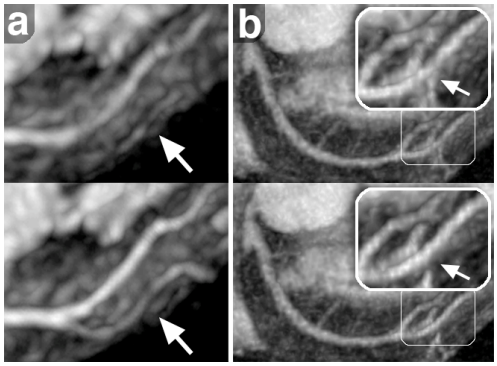

Figure 3. Reformatted MIPs from two patient studies. **(a)** LAD depiction improves with autofocus motion correction (bottom) compared to bulk translational correction (top) in a 1.25-mm-resolution CMRA dataset. **(b)** Depiction of a distal branch of the LAD (insets) improves with autofocus correction (bottom) compared to bulk translational correction (top) in a 0.8-mm-resolution CMRA dataset.

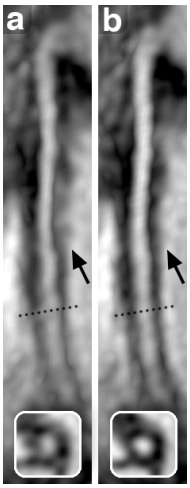

Figure 4. Reformatted MIPs from a 1.25-mm isotropic-resolution volunteer study were reconstructed with **(a)** bulk translational correction measured from 3D iNAVs and **(b)** autofocus motion correction using 36 motion trajectories measured in localized ROIs. RCA depiction and cross-sectional vessel sharpness (insets) improve with autofocus correction.

References [1] Cheng, *et al.* MRM 2012; 68:1785-1797. [2] Moghari, *et al.* MRM 2013; 70:1005-1015. [3] Wu, *et al.* MRM 2013; 69:1083-1093. [4] Addy, *et al.* JCMR 2014; 16:P380. [5] Ingle, *et al.* MRM 2013, early view. [6] McGee, *et al.* JMRI 2000; 11:174-181. [7] Addy, *et al.* 25th MR Angio Conference 2013; 84.